GEOPHYSICS, VOL. 67, NO. 5 (SEPTEMBER-OCTOBER 2002); P. 1548–1557, 10 FIGS.
10.1190/1.1512800

Aquifer heterogeneity from SH-wave seismic impedance inversion

Kevin D. Jarvis* and Rosemary J. Knight‡

ABSTRACT

We collected SH-wave seismic reflection data over a shallow aquifer in southwestern British Columbia to investigate the use of such data in hydrogeologic applications. We used this data set in developing a methodology that uses cone penetrometer data as an integral part of the inversion and interpretation of the seismic data. A Bayesian inversion technique converts the seismic amplitude variations to velocity variations, honoring the probabilities of the priors and adhering to a geologically reasonable sparseness criterion. Velocity measurements acquired with the cone penetrometer provide velocity profiles and vertical seismic profiling (VSP) data, all of which are valuable in properly constraining the Bayesian inversion. The differentiation of lithologies (in this data set, sand and clay) is accomplished by first using a normalization procedure to remove the impact of effective stress, which dominates the velocity variation in the upper 10 to 20 m. The final transformation of seismic velocities to void ratio for the sand-dominated regions is made using laboratory-derived measurements; it provides an image of the heterogeneity of the near-surface aquifer.

INTRODUCTION

A critical part of many groundwater or environmental studies is obtaining quantitative information about the hydrogeologic properties of groundwater aquifers. Numerous techniques have been developed to provide such information; these techniques vary in terms of the scale and accuracy of the measurement. Most of the commonly used methods of subsurface hydrogeologic testing (e.g., tracer tests, pumping tests, slug tests) require a wellbore. Wellbores can be expensive to drill, so there are often too few wells to provide good spatial coverage. In addition, there can be problems associated with the invasive nature of this form of testing—of particular concern in characterizing contaminated regions. An alternative approach is to develop geophysical methods as a means of imaging or sampling the subsurface noninvasively.

Hydrogeologists have recognized the benefits that can be gained by having seismic data from a subsurface region of interest. A synthetic model study by Copty et al. (1993) demonstrates that sparsely sampled permeability and pressure data can be combined with densely sampled seismic velocity data to invert for densely sampled permeability. A relationship between P-wave velocity and permeability developed by Marion et al. (1992) makes a connection between seismic and hydraulic properties. In general there does not exist a unique relationship between velocity and permeability, so two other studies have avoided this difficulty by developing ways of calibrating and incorporating the seismic information. McKenna and Poeter (1995) use crosshole seismic tomographic data to identify certain ranges in P-wave velocity values with distinct hydrofacies. Permeabilities were assigned to the units using measurements from cores and packer tests. Hyndman and Gorelick (1996) also define distinct subsurface zones based on measured seismic velocities and assign uniform hydraulic properties to these zones using information from inverting tracer test data.

The basic concept behind all of these studies is the idea that the subsurface can be divided into regions, each with a distinct range of seismic velocity. These regions, defined by their seismic properties, can then be assigned hydraulic properties. Regardless of the specific methodology followed in using seismic data for hydrogeologic applications, all studies to date illustrate the importance of two key steps: (1) obtaining an accurate model of the velocity variation in the subsurface and (2) providing the link between velocity and hydraulic properties.

Obtaining velocity information from seismic data can take two approaches. One approach is to use existing boreholes to carry out crosshole tomographic experiments. This procedure requires cased boreholes in the study area. In addition to being relatively expensive, cased boreholes pose risks in

Manuscript received by the Editor June 16, 2000; revised manuscript received January 30, 2002.
*Formerly University of British Columbia, Department of Earth and Ocean Sciences, 2219 Main Mall, Vancouver, British Columbia V6T 1Z4, Canada; presently Whytecliff Geophysics Ltd., 2618 Oxford St., Vancouver, British Columbia, V5K 1N3 Canada. E-mail: whytecliff@canada.com.
‡Formerly University of British Columbia, Department of Earth and Ocean Sciences, 2219 Main Mall, Vancouver, British Columbia V6T 1Z4, Canada; presently Stanford University, Geophysics Department, Stanford, California 94305. E-mail: rknight@pangea.stanford.edu.

contaminated aquifers. A second approach uses surface seismic data. Surface seismic techniques are noninvasive and provide a detailed 2-D or 3-D image of the subsurface.

Our study focuses on the use of surface-based shear-wave (S-wave) seismic reflection data as a means of describing the heterogeneity of a sand aquifer; specifically, we use the seismic data to obtain a void ratio model of the aquifer. While there have been a number of studies illustrating the usefulness of compressional-wave (P-wave) reflection data for near-surface applications (e.g., Steeples and Miller, 1990; Büker et al., 1998), surprisingly little work has been done on the use of S-wave data, with the exception of studies by Hasbrouck (1991), Hunter, Pullan et al. (1998), and Carr et al. (1998). An obvious advantage of S-wave data in many shallow environments is improved vertical resolution, which is taken to be one-fourth of the dominant wavelength (Sheriff, 1989). In water-saturated sediments the S-wave velocity is generally much less than the P-wave velocity, resulting in a smaller wavelength (the velocities differ by a factor of 8, and the dominant S-wave frequency is typically one-half of the dominant P-wave frequency). Another significant difference between P-wave and S-wave techniques is the lack of sensitivity of the shear modulus to fluid saturation. This characteristic of S-wave techniques results in a larger change in S-wave velocity compared to P-wave velocity for a given variation in void ratio or lithology.

The first issue we address is the critical step of obtaining an accurate velocity model from the collected data. Interval velocities can be obtained by applying the Dix equation (Dix, 1955) to the stacking velocities, but this technique assumes horizontal reflectors and is prone to large unconstrained errors. We chose an impedance inversion algorithm (Sacchi and Ulrych, 1996) which uses seismic trace amplitudes. To obtain usable results from impedance inversion, velocity constraints are required that are typically obtained by velocity logging in a nearby cased borehole. In this study we obtained the near-surface velocity information, required for the inversion, from the seismic cone penetrometer. This is an attractive alternative to the use of expensive, invasive borehole logging, and it is ideally suited for the inversion of shallow surface seismic data.

The second issue, if seismic methods are to be used for hydrogeologic applications, is to convert the velocity model to a map of hydrogeologic parameters of interest. Our approach involved information derived from the cone velocity data and from laboratory measurements, the final product being a lithology and void ratio model of the aquifer system.

Our overall objective in this study was to investigate the optimal way of using shear-wave seismic reflection data to estimate hydraulic properties. A novel aspect of the methodology was the use of cone penetrometer data as an integral part of inverting the surface seismic data and interpreting the velocity model. We found that cone-measured data can contribute significantly to the use of near-surface seismic data for hydrogeologic applications.

GEOLOGIC SETTING

This investigation was carried out on the Fraser River delta, southwestern British Columbia, Canada, at the Kidd2 research site (Figure 1). This site has been the focus of a number of studies, including the Canadian Liquefaction Experiment (CANLEX), which resulted in a large number of cone penetrometer holes and the retrieval of three frozen cores for laboratory measurements (Hofmann, 1997). A number of hydrogeologic experiments have also been carried out at the site (e.g., Wood, 1996) by using a pumping well, multilevel sampling wells, and zone-specific piezometer installations. Neilson-Welch (1999) used the multilevel sampling wells to obtain groundwater chemistry data, which were combined with measured hydrogeologic parameters to develop a groundwater flow model. The Geological Survey of Canada has obtained cores, participated in geotechnical studies, and performed geophysical surveys at the site (Hunter, Burns et al., 1998) in an ongoing effort to study the liquefaction potential and earthquake site amplification effects of the Fraser delta. Thanks to the cooperation of BC Hydro, an ideal field research site was established to carry out both hydrogeological and geophysical investigations.

The stratigraphy of the site is associated with the progradation of the Fraser delta during the Holocene. The sediments at the surface consist of fine-grained floodplain and upper intertidal material (Clague et al., 1983). Underlying the near-surface sediments are a sequence of sands and silts representative of river-channel deposits interbedded with intertidal sands. Some of the channels cut down into the underlying sediments by as much as 20 m (Clague et al., 1983). A sequence of former delta-slope sands and silts underlies the channel deposits. These sediments show both lateral and vertical variations in textures that are attributed to shifting distributary channels (Clague et al., 1983). Beneath the sand–silt sequence lie fine silt and clay sediments deposited in a marine basin environment. At the base of the Holocene sediments is the Pleistocene till, which is composed of compacted glacial sediments.

Using work by Wood (1996) and Neilson-Welch (1999), we developed a simple model of the site: floodplain and intertidal silt and clay in the upper 4 to 5 m; underlying river-channel, intertidal, and former delta-slope sands forming the aquifer to a depth of 21 to 23 m; marine clays and silts to a depth of 49 to 52 m; and Pleistocene till underlying the entire sequence. Core analysis by Wood (1996) revealed a series of fining-upward sequences within the sand aquifer that divide the aquifer into upper and lower zones. The upper aquifer represents the uppermost fining-upward sequence and has a depth range of 5 to 13 m. The lower aquifer has a depth

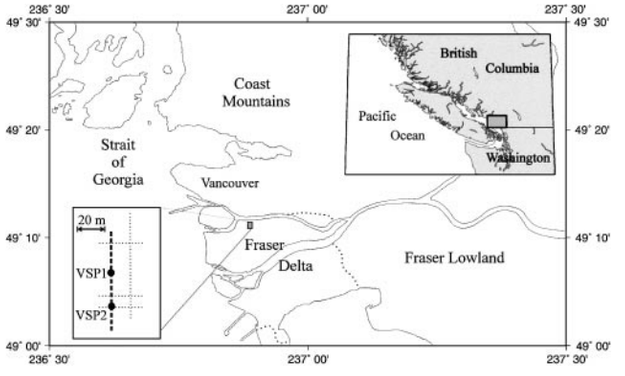

FIG. 1. The Kidd2 research site on the Fraser River delta with the grid of SH-wave CDP seismic data (dotted lines) and the two VSPs, labeled VSP1 and VSP2, used for impedance constraints. Seismic line 20, used in the inversion, is highlighted.

range of 13 to 22 m. The upper aquifer has a number of very fine sand and silt layers up to 10 cm thick that are probably related to river-channel deposition along with a few thin zones (1 to 2 cm) of clay. The lower aquifer tends to be uniformly composed of sand. Hofman (1997) measured the void ratio in the frozen cores retrieved predominantly from the lower aquifer (12 to 17 m) and obtained values ranging from 0.88 to 1.12. The water table is approximately 1 m below the surface at the site, with some variation in depth as a result of tidal influences.

SH-WAVE SEISMIC REFLECTION DATA

Data acquisition

The common depth point (CDP) shear-wave seismic data were collected in June 1996 using a 24-channel Geometrics SmartSeis seismograph, 48 Geo Space horizontal geophones (20DM-28 Hz) attached to CDP spread cables, and an I/O RLS-100 roll switch. An end-on shooting configuration was used with a geophone and source spacing of 1 m, giving a far offset of 24 m and 1200% subsurface coverage. The seismic source consisted of a 35-kg steel block with metal fins attached to the base to increase the source coupling. The SH-waves were generated by swinging a 5-lb sledgehammer against the sides of the block. To further increase source coupling, the person swinging the hammer stood on the block.

The SH-wave technique was used to minimize mode conversions and P-wave interference. An average of ten hammer blows were stacked for each record to improve the S/N ratio and remove the effects of the occasional misdirected blow. Data were recorded with blows in opposite directions to allow for subtracting the records to further reduce P-wave interference and provide additional S/N enhancement of the SH-waves. A total of five lines of SH-wave seismic data were acquired and processed, covering 420 m. The locations of these lines are shown in Figure 1. We will examine line 20, a 100–m north–south line (highlighted in Figure 1).

Data analysis and processing

The seismic data were processed using a Unix-based seismic processing system installed on a Sun workstation network. The processing flow was the same as that commonly used in the petroleum industry and consisted of spherical divergence correction, bandpass filtering, record subtraction, deconvolution, NMO removal, residual statics, stacking, and migration. Refraction statics were not applied to the data because the elevation at the site varied by <1 m. Most large velocity variations in the near surface are confined to the upper 2 m, which can be dealt with adequately by residual statics.

A spherical divergence correction was applied using a time-scaling function with a power of 2.0. The data were bandpass filtered (25/50–150/400 Hz) using a minimum-phase Butterworth filter. The record subtraction process was preceded by applying a trace-to-trace amplitude balance. The surface-consistent deconvolution used both shot and receiver gathers, with trace-by-trace editing afterward to remove the noisy segments. The elevation statics compensated for a topographic variation of <1 m across the site. A semblance velocity analysis was used iteratively with surface-consistent residual statics. The mute function tended to be quite conservative to ensure that the amplitude variations at shallow depths did not dominate the stack. The data were migrated using an interval velocity model based on the extensive data from the site.

Two shot profiles from both ends of the line are shown in Figure 2. These profiles represent the data quality after subtracting the records. Hyperbolic reflections are obvious from 0.10 to 0.30 s, and a reflection from the top of the Pleistocene till is present at approximately 0.5 s. Additional reflections cannot be seen at this stage of the processing; the stacking process is needed for enhancement.

The migrated data set is shown in Figure 3. The reflectivity variations on the seismic section are directly related to the dominant lithologic units. The upper 0.3 s has relatively high reflectivity from lithologic variations within the sand aquifer. In particular, the upper aquifer zone shows the highest reflectivity. From 0.3 to 0.5 s the reflectivity is reduced because of a lack of lithologic variation in the underlying marine clay–silt sequence. The reflection off the Pleistocene till is the most dominant coherent reflection at 0.5 s, which results from a very large velocity change (Hunter, Burns et al., 1998).

A large channel is obvious within the sand unit, extending from CDP 1112 to the northern end of the line at approximately 0.15 s. This channel has not been observed or inferred by the other investigations carried out at the site. The channel is interpreted as a distributary channel because it lies completely within the upper aquifer, which is the region most likely to be dominated by distributary channels. Other reflections within the aquifer are believed to correspond to the interfaces noted by Clague et al. (1983) that were attributed to variations in the texture of the delta slope materials.

A relatively strong horizontal reflection is obvious in the data at approximately 0.35 s. This reflection falls within the marine silt and clay region where no significant reflections are expected. One possibility is that this reflection may be a multiple. The source of this multiple is not known, but it is most likely an interbedded multiple from within the aquifer.

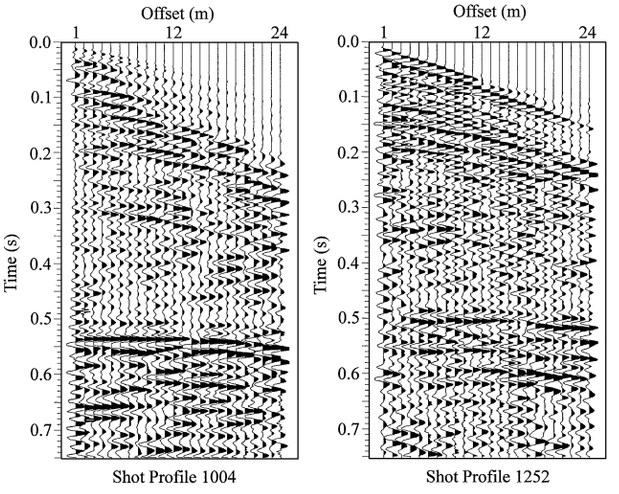

FIG. 2. Two representative shot profiles from line 20 after application of gain, trace balancing, and record subtraction. Shot profile 1004 is at the south end of the line, and shot profile 1252 is at the north end.

SEISMIC CONE PENETROMETER DATA

The cone penetrometer is a minimally invasive technology developed by geotechnical engineers for rapid in-situ site characterization. A steel rod with a cone-shaped tip is pushed into the ground hydraulically while making measurements with sensors mounted close to the tip (Robertson et al., 1986). The technique works extremely well in deltaic deposits consisting of sand, silt, or clay. In the past, most of the data obtained with the cone penetrometer consisted of standard cone parameters such as tip resistance, sleeve friction, and pore pressure response. Over the years additional sensors such as geophones or accelerometers have been added to the cone to measure seismic arrival times. These seismic cone penetrometers are referred to as SCPTU (Robertson et al., 1986). Conventionally, shear-wave velocities have been determined from first arrival or first crossover times of polarized shear waves generated at the ground surface during pauses in penetration in an SCPTU sounding.

Jarvis and Knight (2000) outline an extension of the standard SCPTU sounding to carry out vertical seismic profiling (VSP). The VSP survey is a way to obtain high-resolution reflection images of the subsurface using a subsurface sensor (typically in a borehole) and surface seismic source. The cone penetrometer is particularly well suited to VSP surveying because of increased coupling of the sensor, decreased cost when compared with conventional borehole VSPs, and fewer unwanted wave arrivals such as tube waves.

In this study the cone VSP data were used in two ways to help invert the surface seismic data. The determined velocities were essential for obtaining the initial velocity model of the subsurface that provides the constraints for the inversion of the surface seismic data. In addition the VSP data provide a way to identify the seismic waveform (another key constraint for the inversion). A third use of the VSP data was in the interpretation stage, where the observed variation in velocity with depth was used to remove the effect of effective stress on the velocity model.

Data acquisition

The cone penetrometer has been used extensively in a number of other studies at the Kidd2 site. Most of the cone holes have acquired data associated with standard geotechnical parameters such as tip resistance, sleeve friction, and pore pressure. Velocity data have been acquired in very few holes. In this investigation the cone accelerometers were used to obtain near-surface VSP data, as described in detail by Jarvis and Knight (2000).

Two shear-wave VSP surveys, referred to as VSP1 and VSP2, were conducted along line 20, located as shown in Figure 1, using the cone penetrometer truck from the Department of Civil Engineering at the University of British Columbia. A large sledgehammer struck against the baseplate of the truck was used as the source of SH-waves, and a cone-mounted accelerometer was used as the receiver. Bidirectional hammer blows and record subtraction were also used to optimize the signal. The data were recorded using a Nicolet oscilloscope with 15-bit data digitizing and storage capability. The depth levels at which the cone was stopped to record VSP data were chosen to minimize field time and spatial aliasing. The truck engine (which must be running to power the hydraulic system) was turned off before every measurement to reduce the noise.

Interval velocity logs

The interval velocities are obtained from the first arrivals of the VSP surveys. The interval velocity logs from the VSP surveys are shown in Figure 4a. Each VSP trace is recorded at a particular depth, and the arrival times are used to calculate the

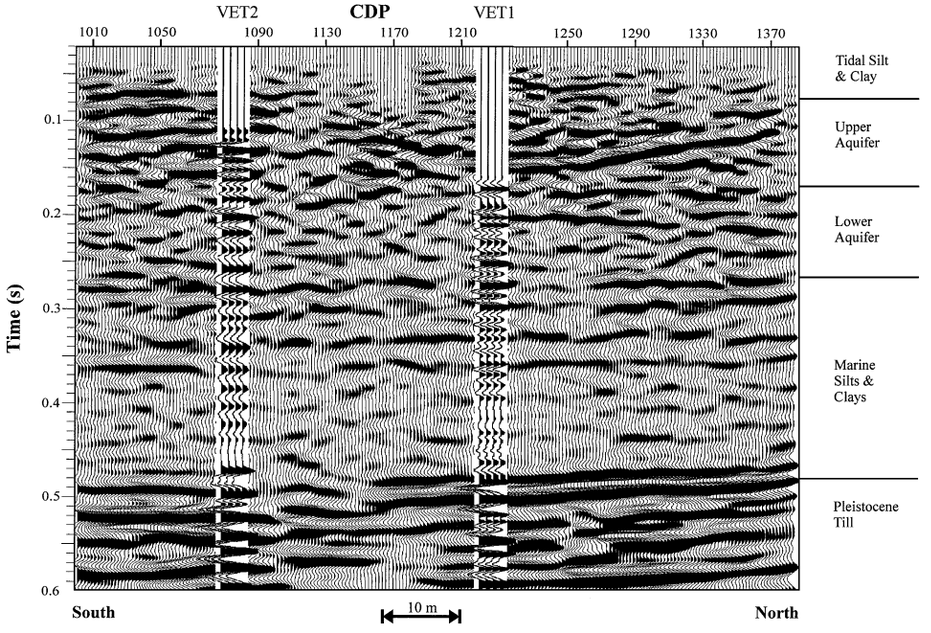

FIG. 3. The migrated SH-wave seismic reflection data (line 20) that were used as input to the seismic impedance inversion. The VETs are shown in their respective locations.

interval velocity between adjacent depth recordings. The accuracy of the interval velocities is dependent on the accuracy of picking the arrival time as well as the accuracy of the assigned depths. The original data were recorded at a sample interval of 0.5 ms, which is adequate to record the frequencies of the data but insufficient for arrival-time picking. To increase accuracy, the data were subsampled down to 0.05 ms. The depths are based on the lengths of rod used by the cone penetrometer, which are machined to very close tolerances and should be accurate to within 1 mm. Note that the first arrivals (and interval velocities) could have been obtained using standard seismic cone measurement techniques without recording complete VSP traces.

VSP data analysis and processing

In addition to the use of the first arrivals in the VSP data to obtain information about subsurface velocities, the VSP data also provided a way of defining the seismic wavelet in the surface CDP seismic data. The seismic wavelet is a required input to the impedance inversion algorithm. The VSP data set processing followed a generally accepted flow (as outlined by Hardage, 1985). The main objective of the processing was to separate the upgoing and downgoing wavefields and to improve the signal bandwidth using deconvolution. The processing, detailed in Jarvis and Knight (2000), consisted of singular value decomposition, minimum phase deconvolution, match filtering, and f–k filtering. The final step involved stacking the data to create the VSP extracted traces (VETs). The VETs for VSP1 and VSP2 are shown in Figure 3 (VET1 and VET2).

For this particular investigation the VETs played a critical role in allowing us to characterize the wavelet of the S-wave surface seismic data. At a subsurface location sampled by both VSP and CDP data, we were able to determine the phase shift that had to be applied to the migrated CDP data to match the known zero phase of the VETs. This filter was then applied to all of the CDP data, shifting the phase of the embedded wavelet to zero.

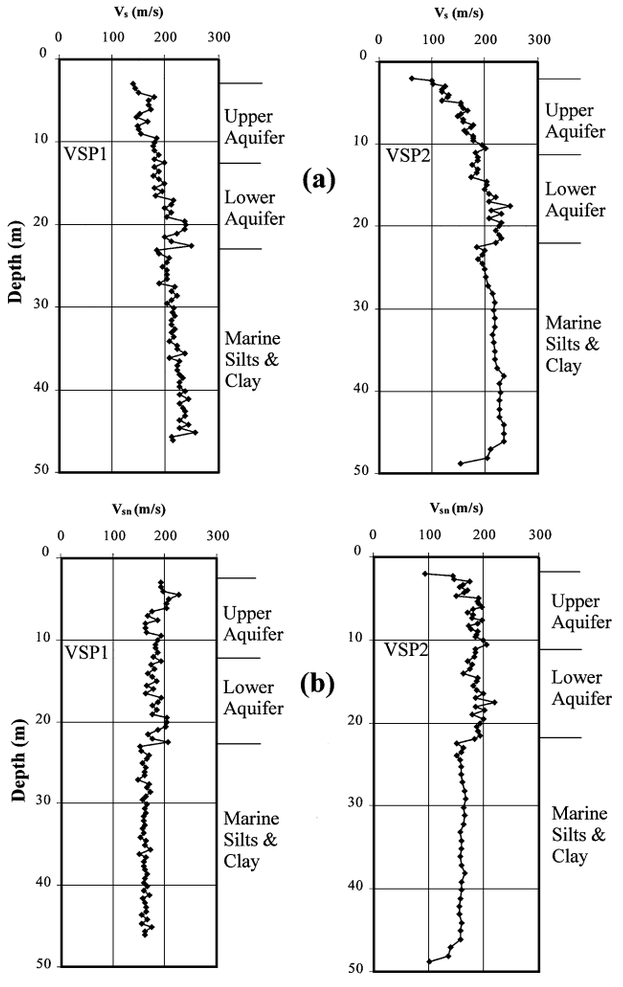

FIG. 4. (a) Interval velocity logs from the two seismic cone penetrometer holes (VSP1 and VSP2). (b) The normalized interval velocity logs. The sand unit of the upper and lower aquifers is clearly differentiated (based on velocity) from the underlying clay–silt unit.

IMPEDANCE INVERSION OF SHEAR-WAVE DATA

Seismic impedance is the product of density and seismic velocity. The amplitude of seismic reflections is from the variation in seismic impedance across a subsurface interface. The seismic impedance inversion is in essence a seismic reflectivity inversion from which the seismic impedance can then be calculated.

Many different techniques have been used to invert seismic data into impedance (e.g., Lines and Treitel, 1984; Tarantola, 1984). The inversion approach that we used was developed at the University of British Columbia by Sacchi and Ulrych (1996). It utilizes a Bayesian technique whereby a priori information and associated error are incorporated into the inversion. The convolutional model of a seismic trace is assumed, where the seismic trace is equal to the convolution of a reflectivity series and a wavelet plus random noise (assumed to be Gaussian). Impedance is obtained by integrating the reflectivity series. Constraints on the impedance will have associated errors that are also assumed to be Gaussian. These errors are from inaccuracies or uncertainties in impedance measurements.

The inversion of the seismic data uses a nonlinear conjugate gradient algorithm (Sacchi and Ulrych, 1996). The output reflectivity model relies on maximizing the a posteriori probability density function (MAP solution). This Bayesian approach results in a reflectivity model that honors the probabilities of the priors and adheres to a sparseness criterion (L1norm). The final impedance model was obtained by integrating the reflectivity model. Our seismic impedance model assumes that the density is relatively constant with depth. For this particular site, the water table is within 1 m of the surface, and all sediments are saturated; so this is taken to be a reasonable assumption. With a constant density assumption the impedance model is equivalent to an SH-wave velocity model.

The input velocity model is shown in Figure 5. The model is based on three control points. The first control point is the location of VSP2 at CDP 1082, and the second control point is the location of VSP1 at CDP 1216. At these control points interval velocity data from the seismic cone penetrometer are available from a depth of 3 m down to the top of the Pleistocene till. The velocity of the till had to be estimated because the cone

could not penetrate it. Hunter, Burns et al. (1998) determined that, the velocity of the Pleistocene till is at least double the velocity of the overlying deltaic sediments; our model reflects this large increase in velocity.

Because of the variations to the north of CDP 1216, a third control point was inserted at the north end of the line. At CDP 1373 the data from a cone hole were available. Unfortunately, there were no velocity data, only tip resistance and sleeve friction logs. In the upper 10 m, where we interpreted there to be the low-velocity edge of a channel, velocities were obtained from the measured tip resistance using an empirical relationship between velocity and tip resistance established with the data from VSP1 and VSP2. Below 10 m the velocities from VSP1 were used. The reflection time (on the CDP data) at the base of the aquifer and the top of the Pleistocene till were used as a guide to position the VSP1 velocities.

A comparison of the input and output velocity models is shown in Figure 6. The two sets of velocity traces represent the location of the two VSPs, where the input velocity model has been obtained from the interval velocity logs. The dashed line is the input velocity model, and the solid line is the output from the inversion. The increase in velocity at the Pleistocene till is readily apparent at a depth of 50 m. The trends in the velocities are very similar, thereby demonstrating how large-scale velocity changes are honored by the inversion. The variations in the output model below the top of the Pleistocene till result from the presence of a series of closely spaced reflections in the seismic data set, which are likely to be associated with velocity variations within the Pleistocene till. However, no velocity information is available to properly constrain the inversion of this zone, so the accuracy of the output model in this region is questionable.

One test of the success of any inversion is the ability to reproduce the input data. The derived impedances can be converted into reflection coefficients and convolved with the source wavelet to create a seismic data set. This data set is shown in Figure 7. When compared with Figure 3, there are very few differences between the two data sets, demonstrating that the inversion output is a viable solution.

The output velocity model from the inversion is shown in Figure 8. The velocity variation is similar in form but differs in detail when compared to the input model. The continuity of the velocities in the input model results from the interpolation of three control points. The output model does not show this same continuity because the recorded changes in seismic amplitudes have been honored by the inversion.

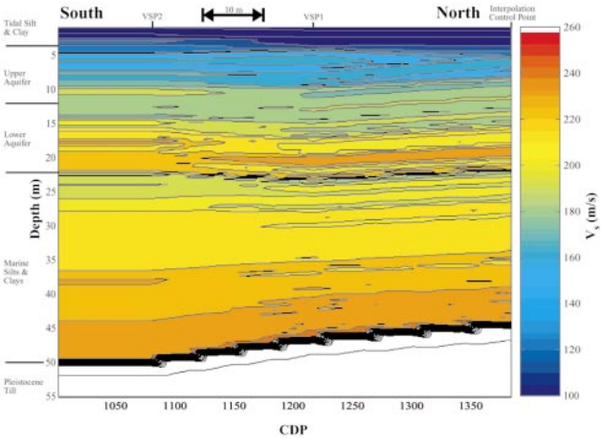

FIG. 5. Input velocities to the seismic impedance inversion.

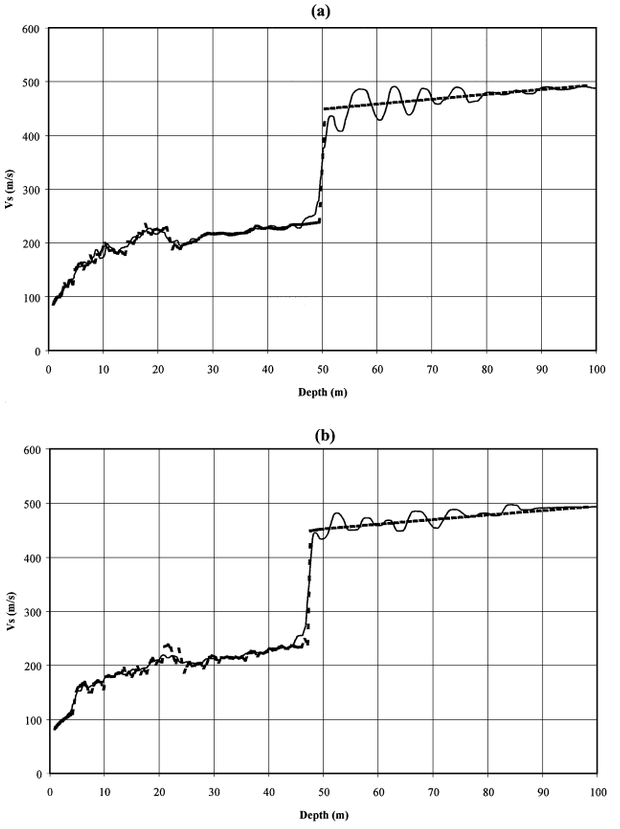

FIG. 6. A comparison of the velocity logs from (a) VSP2 and (b) VSP1 to the output from the seismic impedance inversion. The dashed line is the velocity log; the solid line is the inversion output.

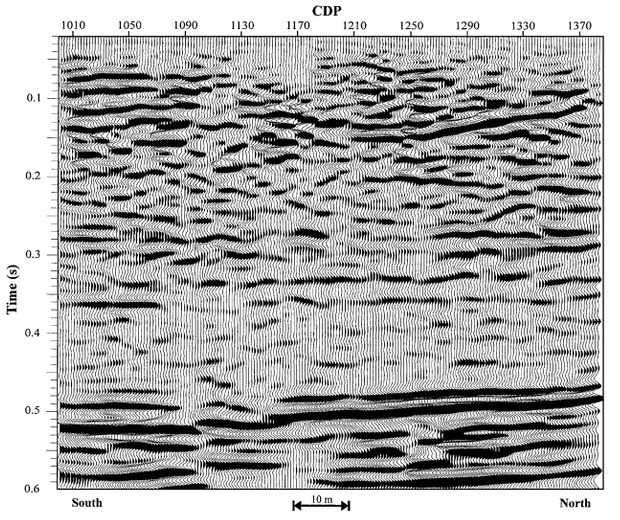

FIG. 7. The output impedance model convolved with the source waveform. These data closely match the input data shown in Figure 3.

Our working hypothesis is that the variation in seismic velocity of the subsurface can be used to map heterogeneity in the hydraulic properties of the aquifer. In Figure 8 we acquired, through inversion of our collected surface seismic data, a model of seismic velocity. The next step was to transform this into an image showing sand and clay regions. Separating the sand unit and using laboratory measurements made it possible to determine spatial variability in the void ratio of the sand.

DIFFERENTIATING LITHOLOGY USING THE VELOCITY MODEL

A desirable objective in using seismic data for hydrogeologic studies is to relate the measured velocity to permeability. However, the relationship between permeability and velocity is not straightforward. The use of laboratory-derived relationships, such as that presented by Marion et al. (1992), requires key assumptions about the microstructure of the in-situ material, e.g., a sand framework with constant intergranular void ratio. Alternatively, some means of calibrating field-measured velocity data with field-measured permeability is required, as in the study by McKenna and Poeter (1995). In our study, given insufficient knowledge about the subsurface materials to accurately obtain permeability information, we elected to use the velocity model to determine variation in void ratio. The void ratio is a measure of the volume of water in a saturated aquifer and is one of the parameters that determines permeability.

As with most rock physics relationships, the relationship between velocity and void ratio can be better defined if applied to single lithologic units. In this study we were primarily interested in the sand aquifer. To identify the distinct lithologic units in our velocity model, we had to first remove the influence of effective stress, which increases velocity with depth and dominated the output model (Figure 8). Correcting for effective stress allowed us to identify the individual lithologic units and clarified the velocity variation within the sand that was related to variation in material properties.

Correcting for effective stress in velocity data

A complicating factor in the interpretation of any near-surface velocity measurement is effective stress, which in general increases the shear-wave velocity with depth. Removing this effect from the measured velocity is a procedure referred to as stress normalization.

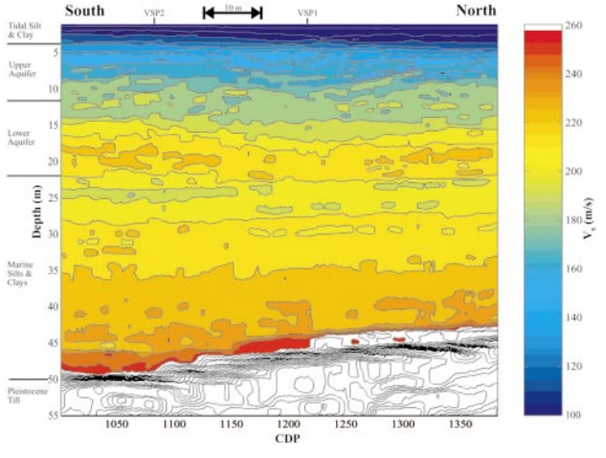

FIG. 8. Velocity output from the seismic impedance inversion.

The concept of stress normalization was developed by geotechnical engineers to help identify lithologies based on seismic velocity. Robertson et al. (1992) used a formula based on lab studies by Hardin and Drnevich (1972). The normalized velocity V_{sn} is given by

$$V_{sn} = V_s\left(\frac{P_a}{\sigma_v'}\right)^{0.25}, \tag{1}$$

where V_s is the measured shear-wave velocity, P_a is the atmospheric pressure (~100 kPa), and σ_v' is the vertical effective stress [obtained by multiplying the unit weight of soil (18 kPa/m) by the depth and subtracting the hydrostatic pressure]. It has been suggested that the value of the stress exponent is not a constant of 0.25 but is variable and possibly site specific. Other researchers (e.g., Tokimatsu et al., 1991; Lee and Campbell, 1985) have found exponents ranging from 0.31 to 0.46 in their normalization function.

Because of the variability of the stress normalization exponent, we used the local velocity data from the interval velocity logs to derive site-specific normalization parameters. Referring to Figure 4a, the increase in velocity from effective stress is most obvious in the upper 10 m. The normalization function, which we chose to use, was determined by examining the velocities within the thick, uniform clay layer interpreted, based on CPT data, to extend from 22 to 50 m. The clay layer was apparent on the cone penetrometer data with low tip resistance and high friction ratio (Wood, 1996). The correct normalization function should produce a constant normalized velocity in a layer of uniform lithology.

We found that the normalization function used by Robertson et al. (1992) was unsatisfactory for this data set. The problem with this particular relationship is that it produces an unrealistically large normalized shear-wave velocity close to the surface where σ_v' is very small. At the surface where σ_v' is zero, V_{sn} is predicted to be ~$2V_s$. Therefore, a modified form of this expression was used to normalize the velocity data:

$$V_{sn} = V_s\left[\frac{P_a}{\sigma_v' + k}\right]^{0.3}, \tag{2}$$

where k is a constant that provides an offset of the velocity normalization function at the surface. For this study k was taken to be 10 kPa. Lee and Campbell (1985) also recognized the need for a constant (k) to account for the nonlinear intersection of shear-wave velocity at the ground surface. The stress exponent was increased to 0.3 partly to compensate for the shifting of the exponential function and ultimately to provide the best normalization function for this site. The quality of the normalization function was evaluated by ensuring that the clay zone velocities fell within a relatively constant range and the sand aquifer velocities exhibited neither overcorrection nor undercorrection of the stress effect.

The normalized velocity data are shown in Figure 4b. The differentiation of velocity between the clay-dominated and sand-dominated units is now apparent. The clay-dominated unit (below 22 m) has a constant normalized velocity of approximately 160 m/s. The sand aquifer (5 to 22 m) has a higher normalized velocity ranging from 160 to 210 m/s. For purposes of separating

the section into sand and clay, we selected 170 m/s as the cut-off; this is the maximum normalized velocity found within the clay-dominated unit.

The normalized output model is shown in Figure 9. The upper and lower bounds of the aquifer are readily apparent on the color plot, with a scale chosen to make the high-velocity silts and sands appear red and yellow and the low-velocity clay-rich material to appear blue and green. The scale focuses on the aquifer velocities; the large increase in velocity at the Pleistocene till is off the scale and is shown in white. The base of the sand channel in the upper 10 m is marked by a low-velocity zone which probably represents a fine-grained silt or clay zone.

The impedance inversion results demonstrate that impedance inversion can be used to map the velocity variations within a near-surface region. The output is highly dependent on the quality of the input, and the absolute velocities will still have error associated with them. The relative variations should be valid and are related to the amplitude variations on the input seismic data. Having removed the stress effect by normalizing the output velocities, we used normalized velocities to differentiate lithologies that can now be interpreted to obtain information about void ratio.

Void ratio in sand aquifer

The primary objective of this study was to develop a means of using surface seismic data to delineate the heterogeneity in the properties of a sand-dominated aquifer. The profile of shear-wave velocity output from the impedance inversion provides insight into the variations in the aquifer. Rather than consider these variations in velocity, we can transform them to illustrate variations in void ratio, a parameter that has more relevance for hydrogeologic investigations.

Previous work (Wood, 1996) describes the aquifer as an upper aquifer composed primarily of sand and silt with a few very thin clay stringers and a lower aquifer composed of a uniform sand. The absence of any significant amount of clay simplifies the interpretation of the velocity data in terms of void ratio. The relationship between S-wave velocity and void ratio in such a system was studied by Hardin and Richart (1963) through an extensive set of laboratory experiments on dry materials ranging from coarse sands to fine silts with void ratios from 0.7 to 1.3. Their laboratory study showed that velocity depends primarily on void ratio and confining pressure, with very little dependence on grain size, resulting in the following empirical relationship:

$$V_s = (104 - 35e)\sigma_o^{1/4}, \tag{3}$$

where e is void ratio and σ_o is confining pressure (in kilopascals).

To adapt this relationship for our study, we needed to account for the saturated state of the aquifer unit. We did this by adding a term to equation (3) to account for the saturated density and defining a revised empirical relationship from the best-fit linear relationship between V_s and e values, generated using the modified form of equation (3). In making this density correction, we assumed a density of 2.65 g/cm^3 for the solid phase. The resulting empirical relationship is

$$V_s = (96 - 37e)\sigma_o^{1/4}, \tag{4}$$

which can also be written as

$$e = 2.6 - \frac{V_s}{37\sigma_o^{1/4}}. \tag{5}$$

Working with the normalized velocity data (Figure 9), the confining pressure was removed as a variable and fixed at the normalizing pressure of 100 kPa. The velocity values, which ranged from 170 to 205 m/s within the sand aquifer, were converted to void ratio values using equation (5). The calculated void ratios ranged from 0.85 to 1.15, in excellent agreement with the range of 0.88 to 1.12 determined from the CANLEX experiment (Hofman, 1997). The final plot of lithology and void ratio is shown in Figure 10. The upper and lower aquifers can be identified by the narrow transition zone from low to high void ratio at approximately 13 m depth. The upper aquifer shows both vertical and horizontal variations in void ratio that most likely represent the wider distribution of sediments expected

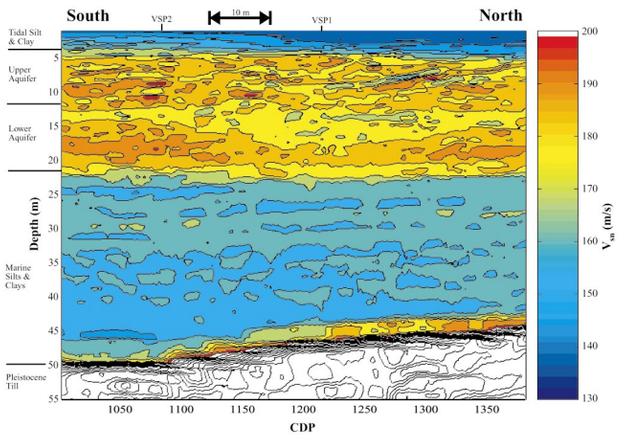

FIG. 9. Normalized velocity output from the seismic impedance inversion. The upper and lower aquifers are clearly identified by yellow and red.

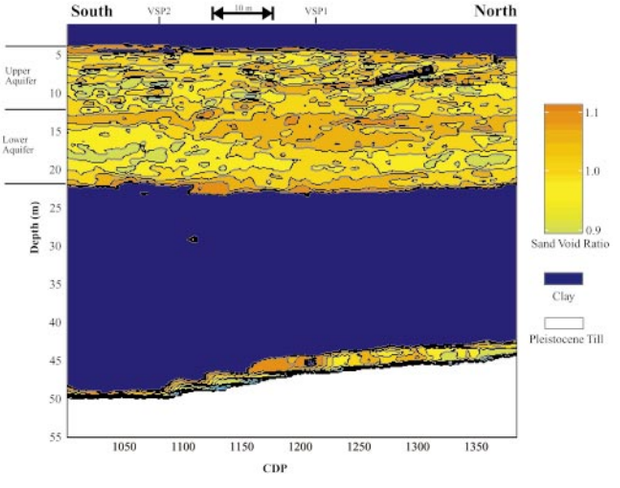

FIG. 10. Lithology–void ratio profile obtained by separating the sand and clay zones using a cut-off velocity of 170 m/s and using equation (5) to obtain the void ratio within the sand aquifer.

in a higher energy near-shore environment. The lower aquifer shows a relatively uniform distribution of void ratio, with void ratio decreasing toward the bottom of the aquifer.

CONCLUSIONS

The use of seismic velocities to quantify hydraulic properties within a near-surface aquifer presents a number of challenges, all of which must be addressed. The first challenge is to obtain reliable velocity values. For near-surface studies, standard velocity measurement techniques such as borehole-based methods are not always available or affordable, so nontraditional techniques such as the cone penetrometer and surface-based reflection seismology must be used wherever possible. The reflection seismic method has the advantage of obtaining very dense subsurface coverage, while the cone penetrometer has the advantage of rapid deployment, reduced cost, and the simultaneous acquisition of other cone logs for stratigraphic interpretation. Employing a Bayesian inversion technique to convert the seismic amplitude variations to velocity variations is a robust method that honors the probabilities of the priors and adheres to a geologically reasonable sparseness criterion.

Once a velocity model has been obtained, it can be used to predict the spatial variation in a hydrogeologic property. The outstanding challenge in this step is determining the correct relationship to use between velocity and the hydrogeologic property. If empirically derived relationships are used, they will be most accurate if they are derived for, and applied to, single lithologic units. The near-surface velocities are dominated by the effect of the rapidly increasing effective stress. This effect must be removed from the velocities to identify the separate lithologic units. The normalization of the velocities accomplishes this task. The analytic function used to normalize the data will depend on the local sediments and their depositional history, so local velocity data are critical to deriving a site-specific normalization function. Once the velocities have been normalized, a separation of lithologies may be possible, depending on the types of sediments under investigation. The availability of core and independent stratigraphic information from the site enables the sediments to be associated with ranges of velocity. As long as the ranges do not overlap, the lithologies can be separated. The final conversion to hydraulic properties can now be achieved on a lithology-specific basis.

This study is an example of the use of SH-wave data to map the spatial heterogeneity in a near-surface aquifer. We have addressed the two key challenges of obtaining a velocity model and transforming it to display variation in lithology and void ratio. The use of measurements made with the cone penetrometer was a novel and critical part of both the inversion and the interpretation of the data. The integration of cone-based measurements with geophysical surface-based measurements extends the capabilities of both of these methods of near-surface characterization and is a promising area for further research.

ACKNOWLEDGMENTS

This research was supported primarily by an NSERC collaborative research grant to R. K. with additional funding obtained from an NSERC research grant. K. J. was also supported by an NSERC postgraduate scholarship. We thank Golder Associates for the use of the Geometrics seismograph, John Howie for the use of the UBC Department of Civil Engineering cone truck, and Mauricio Sacchi for providing the Bayesian impedance inversion algorithm. The field work would not have been possible without the dedicated work of Ian Blumel, David Butler, Christina Chan, Jay Joyner, Jane Rea, Richard Taylor, and Paulette Tercier from the Department of Earth and Ocean Sciences, and Chris Daniel, Heraldo Giacheti, Scott Jackson, and Harald Schrempp from the Department of Civil Engineering.

REFERENCES

Büker, F., Green, A. G., and Horstmeyer, H., 1998, Shallow 3-D seismic reflection surveying: Data acquisition and preliminary processing strategies: Geophysics, **63**, 1434–1450.

Carr, B. J., Hajnal, Z., and Prugger, A., 1998, Shear-wave studies in glacial till: Geophysics, **63**, 1273–1284.

Clague, J. L., Luternauer, J. L., and Hebda, R. J., 1983, Sedimentary environments and postglacial history of the Fraser delta and lower Fraser Valley, British Columbia: Can. J. Earth Sci., **20**, 1314–1326.

Copty, N., Rubin, Y., and Mavko, G., 1993, Geophysical–hydrological identification of field permeabilities through Bayesian updating: Water Resources Res., **29**, 2813–2825.

Dix, C. H., 1955, Seismic velocities from surface measurements: Geophysics, **20**, 68–86.

Hardage, B. A., 1985, Vertical seismic profiling part A: Principles, 2nd ed.: Geophysical Press.

Hardin, B. O., and Drnevich, V. P., 1972, Shear modulus and damping in soils, design equations and curves: J. Soil Mech. Found. Div., Am. Soc. Civil Eng., **98**, 667–692.

Hardin, B. O., and Richart, F. E., 1963, Elastic wave velocities in granular soils: J. Soil Mech. Found. Div., Am. Soc. Civil Eng., **89**, 33–65.

Hasbrouck, W. P., 1991, Four shallow-depth, shear-wave feasibility studies: Geophysics, **56**, 1875–1885.

Hofmann, B. A., 1997, In situ ground freezing to obtain undisturbed samples of loose sand for liquefaction assessment: Ph.D. thesis, Univ. of Alberta.

Hunter, J. A. M., Burns, R. A., Good, R. L., and Pelletier, C. F., 1998, A compilation of shear-wave velocities and borehole geophysics logs in unconsolidated sediments of the Fraser River delta: Geol. Surv. Can. Open File Report D3622.

Hunter, J. A., Pullan, S. E., Burns, R. A., Good, R. L., Harris, J. B., Pugin, A., Skvortsov, A., and Goriainov, N. N., 1998, Downhole seismic logging for high-resolution reflection surveying in unconsolidated sediments: Geophysics, **63**, 1371–1384.

Hyndman, D. W., and Gorelick, S. M., 1996, Estimating lithologic and transport properties in three dimensions using seismic and tracer data: The Kesterson aquifer: Water Resources Res., **32**, 2659–2670.

Jarvis, K. D., and Knight, R. J., 2000, Near-surface VSP surveys using the seismic cone penetrometer: Geophysics, **65**, 1048–1056.

Lee, M. M., and Campbell, K. W., 1985, Relationship between shear-wave velocity and depth of overburden: Meas. and Use of Shear-Wave Velocities, Am. Soc. Civil Eng., Proceedings, 63–76.

Lines, L. R., and Treitel, S., 1984, A review of least square inversion and its application to geophysical problems: Geophys. Prosp., **32**, 159–186.

Marion, D., Nur, A., Yin, H., and Han, D., 1992, Compressional velocity and porosity in sand–clay mixtures: Geophysics, **57**, 554–563.

McKenna, S. A., and Poeter, E. P., 1995, Field example of data fusion in site characterization: Water Resources Res., **31**, 3229–3240.

Neilson-Welch, L. A., 1999, Saline water intrusion from the Fraser River estuary: A hydrogeological investigation using field chemical data and a density-dependent groundwater flow model: M.S. thesis, Univ. of British Columbia.

Robertson, P. K., Campanella, R. G., Gillespie, D., and Rice, A., 1986, Seismic CPT to measure in situ shear-wave velocity: J. Geotech. Eng., **112**, 791–803.

Robertson, P. K., Woeller, D. J., and Finn, W. D. L., 1992, Seismic cone penetration test for evaluluating liquefaction potential under cyclic loading: Can. Geotech. J., **29**, 686–695.

Sacchi, M. D., and Ulrych, T. J., 1996, Bayesian priors for sparse inversion: 23rd Ann. Mtg., Can. Soc. Expl. Geophys., Abstracts, 66–67.

Sheriff, R. E., 1989, Geophysical methods: Prentice-Hall, Inc.

Steeples, D. W., and Miller, R. D., 1990, Seismic reflection methods applied to engineering, environmental and groundwater problems,

in Ward, S. H., Ed., Geotechnical and environmental geophysics, vol. 1: Soc. Expl. Geophys., 1–29.
Tarantola, A., 1984, Linearized inversion of seismic reflection data: Geophys. Prosp., **51**, 332–346.
Tokimatsu, K., Kuywayama, S., and Tamura, S., 1991, Liquefaction potential evauluation based on Rayleigh wave investigation and its comparison with field behaviour: 2nd Internat Conf. on Recent Advances in Geotech. Earthquake Eng. and Soil Dyn., Proceedings, **1**, 357–364.
Wood, E., 1996, Comparison of hydraulic conductivity test methods for the Kidd2 site in Richmond, B.C.: B.S. thesis, Univ. of British Columbia.